JYRKI MIETTINEN[1], VILLE-VALTTERI VISURI[1*], TIMO FABRITIUS[1]

THERMODYNAMIC DESCRIPTION OF TERNARY Fe-B-X SYSTEMS. PART 9: Fe-B-Cu

Thermodynamic descriptions of the ternary Fe-B-Cu system and its binary sub-system B-Cu aredeveloped in the context of a new Fe-B-X (X = Cr, Cu, Mn, Mo, Ni, Si, Ti, V, C) database. The thermodynamic parameters of the other binary sub-systems (Fe-B and Fe-Cu) are taken from earlier assessments. Experimental thermodynamic and phase equilibrium data available in the literature have been used for the optimization of the Fe-B-Cu and B-Cu systems' thermodynamic parameters. The solution phases are described using a substitutional solution model and the compounds (two borides of the Fe-B system) are treated as stoichiometric phases. A good agreement was obtained between the calculated and the experimental thermodynamic and phase equilibrium data.

Keywords: phase diagrams, thermodynamic modelling, thermodynamic database, Fe-based systems, Fe-B-X systems, Fe-B-Cu system

1. Introduction

The current contribution builds upon our earlier started research [1] regarding the development of boron containing an iron-based Fe-B-X database, where boron is treated as a substitutional component. In this paper, the previous contributions of Fe-B-Cr [1], Fe-B-Ni [2], Fe-B-Mn [3], Fe-B-V [4], Fe-B-Si [5], Fe-B-Ti [6], Fe-B-C [7] and Fe-B-Cr-Mo [8] in the Iron Alloys Database (IAD) are extended with a description for the ternary Fe-B-Cu system. The purpose is to develop a thermodynamic database for steels [9], which provides important and practical input data for thermodynamic-kinetic models simulating their solidification [10]. An important technical application of the Fe-B-Cu system is related to its strong tendency to form a liquid miscibility gap, which can be utilized in separating Cu from iron in the steel scrap recycling processes [11].

In this ninth part, thermodynamic descriptions of the B-Cu and Fe-B-Cu systems are made using the experimental thermodynamic and phase equilibrium data from the literature. The binary thermodynamic parameters of the Fe-B and Fe-Cu systems were adopted from Miettinen and Vassilev [1] and Cheng and Jin [12]. The B-Cu system has earlier been assessed by Wang et al. [13] and Zhang et al. [14]. The descriptions pre-sented in [13-14] could not be adopted directly since they apply an interstitial filling of B atoms in the bcc and fcc phases instead of the substitutional filling employed in the Fe-B-X database [1-8]. Although the substitutional filling approach is physically less correct, it causes virtually no error in the calculations, because the solubility of B in the bcc and fcc phases is very low. As demonstrated in the earlier descriptions for Fe-B-X systems [1-8], the substitutional solution model works well also with the liquid phase. Another reason for reassessing the B-Cu system, in relation to the study by Zhang et al. [14], is that our database treats the beta-rhombo-B phase as a substitutional solution phase, whereas Zhang et al. [14] treat it as a sublattice phase formulated as $B_{93}(B,Cu)_{12}$.

2. Phases, modeling and data

Table 1 shows the phases and their modeling in the current Fe-B-Cu assessment. The ternary solution phases (liquid, bcc and fcc) are described with a substitutional solution model [15] while the binary compounds (borides Fe_2B and FeB) are treated as stoichiometric phases.

[1] UNIVERSITY OF OULU, PROCESS METALLURGY RESEARCH UNIT, P.O. BOX 4300, FI-90014 UNIVERSITY OF OULU, FINLAND
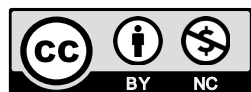
* Corresponding author: ville-valtteri.visuri@oulu.fi

TABLE 1

Phases and their modeling in the current Fe-B-Cu description

Phase	Modeling
liquid (L)	(B,Cu,Fe), substitutional, RKM
bcc_A2 (bcc, ferrite, α-Fe)	(B,Cu,Fe), sublattice, RKM
fcc_A1 (fcc, austenite, γ-Fe)	(B,Cu,Fe), sublattice, RKM
beta-rhombo-B (bet)	(B,Cu), substitutional, RKM
Fe$_2$B	(Fe)$_2$(B), stoichiometric
FeB	(Fe)(B), stoichiometric

RKM = Redlich-Kister-Muggianu (Gibbs excess energy model)

2.1. Solution phases

For a substitutional solution phase of the Fe-B-Cu system, the molar Gibbs energy is expressed as

$$G_m^\phi = x_{Fe}^\phi \, {}^oG_{Fe}^\varphi + x_B^\phi \, {}^oG_B^\phi + x_{Cu}^\phi \, {}^oG_{Cu}^\phi +$$
$$+ RT(x_{Fe}^\phi \ln x_{Fe}^\phi + x_B^\phi \ln x_B^\phi + x_{Cu}^\phi \ln x_{Cu}^\phi) +$$
$$+ x_{Fe}^\phi x_B^\phi L_{Fe,B}^\phi + x_{Fe}^\phi x_{Cu}^\phi L_{Fe,Cu}^\phi + x_B^\phi x_{Cu}^\phi L_{B,Cu}^\phi +$$
$$+ x_{Fe}^\phi x_B^\phi x_{Cu}^\phi L_{Fe,B,Cu}^\phi + {}^{mo}G_m^\phi \tag{1}$$

where R is the gas constant (8.3145 J/K mol), T is the absolute temperature (K), x_i is the mole fraction of component i, ${}^oG_i^\phi$ is the molar Gibbs energy of pure component i in phase ϕ expressed relative to the enthalpy of the component in its stable phase at 298.15K [15, 16], $L_{i,j}^\phi$ is a binary parameter accounting for the interaction between components i and j in phase f, and $L_{Fe,B,Cu}^\phi$ is a ternary interaction parameter of phase ϕ. For these parameters, ${}^oG_i^\phi$ is a function of temperature, and $L_{i,j}^\phi$ and $L_{Fe,B,Cu}^\phi$ $(= L_{i,j,k}^\phi)$ can be functions of temperature and composition. For the interaction parameters, the following composition dependencies [15,17,18] are possible:

$$L_{ij}^\phi = \sum_{m=0}^{m_{MAX}} {}^mL_{ij}^\phi (x_i^\phi - x_j^\phi)^m \tag{2}$$

$$L_{ijk}^\phi = v_i^\phi L_{iijk}^\phi + v_j^\phi L_{ijjk}^\phi + v_k^\phi L_{ijkk}^\phi \tag{3}$$

where m is the degree of the binary parameter (m_{MAX} = maximum degree) and v_i's are composition variables defined as $v_i = x_i + (1 - x_i - x_j - x_k)/3$. The advantage achieved by using the terms v_i as composition variables (instead of mole fractions) is that the sum of the v_i terms is always 1 in multicomponent systems [15]. In the present ternary Fe-B-Cu description, Equation (3) is applied for the liquid phase, whereas no ternary parameters are optimized for the bcc and fcc, phases, due to the very low solubility of boron in them.

The term ${}^{mo}G_m^\phi$ represents the contribution to the Gibbs energy due to the magnetic ordering expressed for solid solution phases, bcc and fcc, as suggested by Hillert and Jarl [19]:

$$^{mo}G_m^\phi = RT \ln(\beta^\phi + 1) \cdot f(\tau) \tag{4}$$

where β^ϕ is a composition-dependent parameter related to the total magnetic entropy and τ is defined as $\tau = T/T_c^\phi$, where T_c^ϕ is

the critical temperature of magnetic ordering. The function $f(\tau)$ takes the polynomial form proposed by Hillert and Jarl [19]. For the liquid phase, of course, ${}^{mo}G_m^\phi = 0$.

2.2. Compounds

The only compounds appearing in the Fe-B-Cu system are the borides Fe$_2$B and FeB of the Fe-B diagram. These are treated as binary stoichiometric phases, as no solubility of a third component has been reported for them. The Gibbs energies of their formation are expressed as

$$^oG_{Fe:B}^\phi = a \, {}^oG_{Fe}^{bcc} + {}^oG_B^{bet} + A + BT \tag{5}$$

where a is a stoichiometric coefficient ($a = 2$ for Fe$_2$B and $a = 1$ for FeB) and ${}^oG_{Fe}^{bcc}$ and ${}^oG_B^{bet}$ are the molar Gibbs energy of pure iron and pure boron in their stable phases at 298.15K, i.e., bcc for iron and beta-rhombo-B for boron [16].

2.3. Experimental data

Table 2 shows the experimental information applied in the optimization of the B-Cu and Fe-B-Cu systems. In the case of B-Cu system, the experimental information is the same as applied in the earlier B-Cu descriptions of Wang et al. [13] and Zhang et al. [14].

TABLE 2

Experimental data of the B-Cu and Fe-B-Cu systems.
The phase equilibrium data of reference [24] were assessed
from the earlier studies of [20-23]

System	Experimental data	Reference
B-Cu	Phase equilibria of the phase diagram	[14,20-24]
	Enthalpy of mixing of liquid alloys at 1,108°C	[25]
	Activity of Cu and B in liquid alloys at 1,517°C, 1,450°C and 1,250°C	[26-28]
Fe-B-Cu	Two isothermal sections (at 1,600°C and 1,250°C)	[11,29]
	Activity coefficient f_{Cu}^B in liquid alloys at 1,600°C	[11,29]

The phase equilibria of the B-Cu system have been studied by several researchers [14,20-24]. The liquidus and the eutectic point were investigated by Zhang et al. [14] using differential thermal analysis, and by Wald and Stormont [20], Rexer and Petzow [21] and Smiryagin and Kvurt [22] using thermal analysis. The solubility of boron in copper was studied by Smiryagin and Kvurt [22] using electronic resistivity measurements and the solubility of copper in boron was studied by Piton et al. [23] using EPMA. Based on the earlier studies [20-23], Chakrabarti and Laughlin [24] made a suggestion for the eutectic temperature and compositions.

The enthalpy of mixing of liquid alloys was investigated

by Kleppa and Sato [25] using high-temperature solution calorimetry. The activity of copper in liquid alloys was studied by Batalin et al. [26] using high-temperature calorimetry, and that of boron was studied by Jacob et al. [27] and Yukinobu et al. [28] using four-phase equilibrium technique and EMF, respectively.

The Fe-B-Cu system was studied by Ono et al. [29] and Yamaguchi et al. [11] using the inductively coupled plasma atomic emission spectrometry (ICP-AES) to detect the B and Cu contents in the Fe-rich liquid phase and the B and Fe contents in the Cu-rich liquid phase.

3. Results and discussion

The thermodynamic description of the Fe-B-Cu system is presented in Table 3. The descriptions marked with a reference code are from earlier assessments, and those marked with O* are optimized in the current study using the literature experimental data shown in Table 2.

The description of the Fe-B system has been previously made by Miettinen and Vassilev [1], and that of the Fe-Cu system has been taken from Cheng and Jin [12]. For the binary B-Cu and the ternary Fe-B-Cu systems, the results calculated

in this work are compared with the original experimental data to verify the optimization as shown in the following subsections. All calculations were carried out with Thermo-Calc software [32].

Figures 1 and 2 show the Fe-B phase diagram calculated by Miettinen and Vassilev [1] and the Fe-Cu phase diagram calculated using the thermodynamic description of Cheng and Jin [12]. The agreement with the experimental data presented in these studies is good.

3.1. System B-Cu

Calculation results by the current study and those of Wang et al. [13] and Zhang et al. [14] are presented in Figures 1-4, together with the experimental data of Table 2. The agreement is reasonably good by each calculation. The IAD results are shown to represent average values between those of Wang et al. [13] and Zhang et al. [14]. The calculated eutectic temperature of 1,014°C in Figures 3 and 4 correlates well with the value of 1,013°C assessed by Chakrabarti and Laughlin [24] and calculated by Wang et al. [13], whereas the temperature calculated by Zhang et al. [14] is a bit higher at 1,027°C. Note also the high

TABLE 3

Thermodynamic description of the Fe-B-Cu system. Thermodynamic data of pure components are taken from [16] unless not shown in the table. Parameter values except for Tc and β are in J/mol. Tc and β are the Curie temperature (K) and the effective magnetic moment (magneton) of a phase, respectively

|	Ref.
liquid (1 sublattice, sites: 1, constituents: B,Cu,Fe)	**Ref.**
$L^L_{B,Cu} = (-2500) + (+16500 - 10T)(x_B - x_{Cu}) + (+38000 - 15T)(x_B - x_{Cu})^2$	O*
$L^L_{B,Fe} = (-133438 + 33.946T) + (+7771)(x_B - x_{Fe}) + (+29739)(x_B - x_{Fe})^2$	[30]
$L^L_{Cu,Fe} = (+35626 - 2.19T) + (-1530 + 1.153T)(x_{Cu} - x_{Fe}) + (+12714 - 5.186T)(x_{Cu} - x_{Fe})^2 + (+1177)(x_{Cu} - x_{Fe})^3$	[12]
$L^L_{B,Cu,Fe} = (-120000 + 50T)x_B + (+200000 + 50T)x_{Cu} + (-233000 + 200T)x_{Fe}$	O*
bcc (1 sublattice, sites: 1, constituents: B,Cu,Fe)	**Ref.**
$^oG^{bcc}_B = {}^oG^{bet}_B + (+43514 - 12.217T)$	[31]
$L^{bcc}_{B,Cu} = L^{fcc}_{B,Cu}$	O*
$L^{bcc}_{B,Fe} = (-50000 + 42T)$	[1]
$L^{bcc}_{Cu,Fe} = (+39676 - 4.732T)$	[12]
$Tc^{bcc} = 1043x_{Fe} - 41.4x_{Fe}x_{Cu}$	[12]
$\beta^{bcc} = 2.22x_{Fe}$	[12]
fcc (2 sublattices, sites: 1, constituents: B,Cu,Fe)	**Ref.**
$^oG^{fcc}_{B:Va} = {}^oG^{bet}_B + (+50208 - 13.478T)$	[31]
$L^{fcc}_{B,Cu} = (+29600)$	[13]
$L^{fcc}_{B,Fe} = (-66000 + 50T)$	[1]
$L^{fcc}_{Cu,Fe} = (+43320 - 6.944T) + (+6069 - 2.837T)(x_{Cu} - x_{Fe}) + (+3629)(x_{Cu} - x_{Fe})^2$	[12]
$Tc^{fcc} = -201x_{Fe}$	[12]
$\beta^{fcc} = -2.1x_{Fe}$	[12]
bet (1 sublattice, sites: 1, constituents: B,Cu)	**Ref.**
$^oG^{bet}_{Cu} = {}^oG^{fcc}_{Cu} + (+5000)$	[13]
$L^{bet}_{B,Cu} = (+34386)$	[13]
Fe₂B (2 sublattices, sites: 2:1, constituents: Fe:B)	**Ref.**
$^oG^{Fe2B}_{Fe:B} = 2{}^oG^{bcc}_{Fe} + {}^oG^{bet}_B + (-78783 + 10.398T)$	[30]
FeB (2 sublattices, sites: 1:1, constituents: Fe:B)	**Ref.**
$^oG^{FeB}_{Fe:B} = {}^oG^{bcc}_{Fe} + {}^oG^{bet}_B + (-70300 + 12T)$	[1]

O* – Parameter optimized in this work
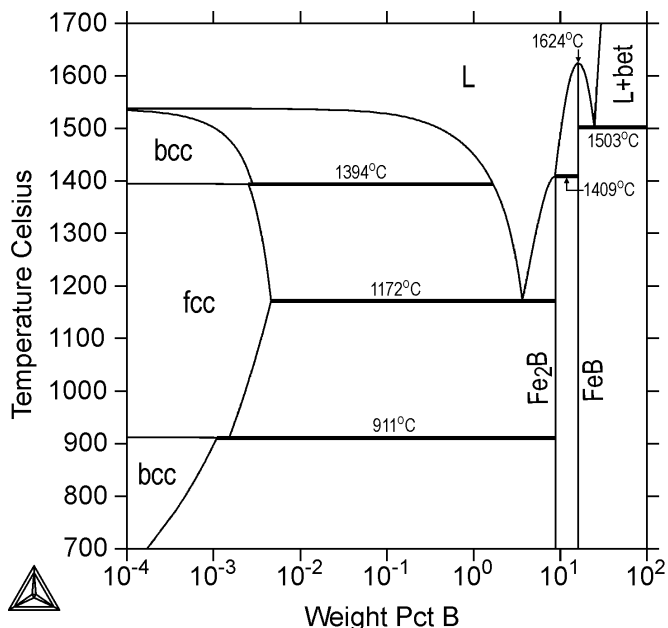
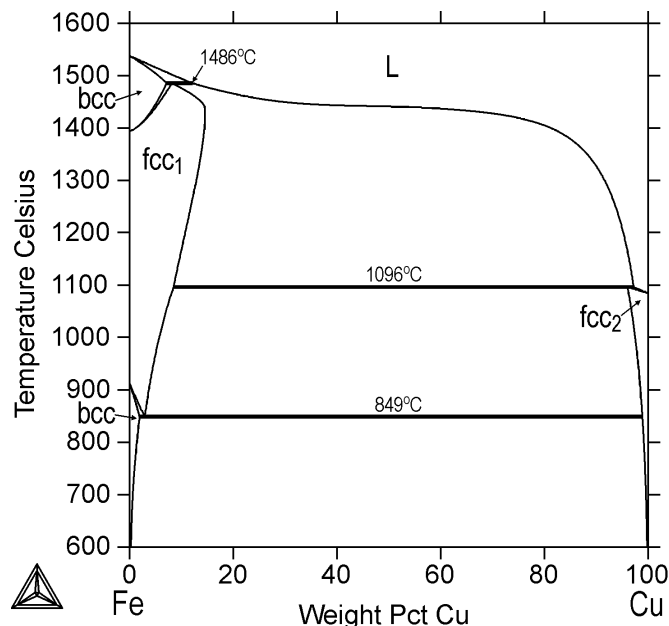Fig. 1. Fe-B phase diagram calculated by Miettinen and Vassilev [1]

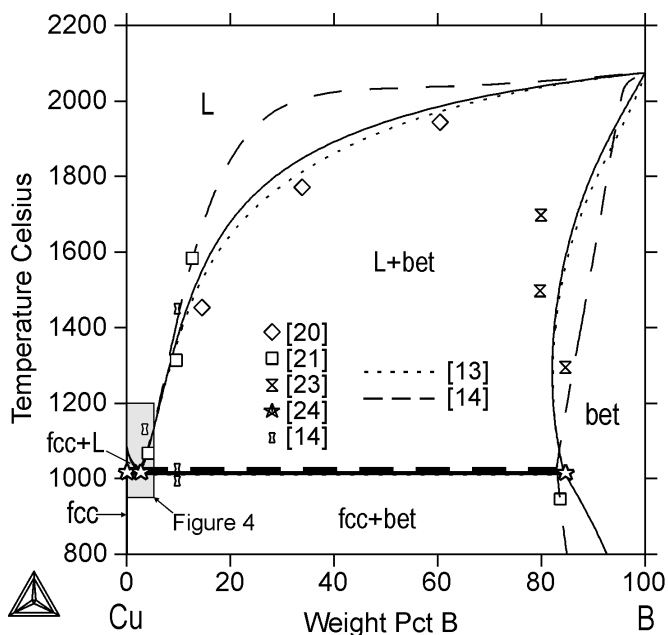Fig. 2. Fe-Cu phase diagram calculated by Chen and Jin [12]

Fig. 3. The calculated B-Cu phase diagram, with experimental [14,20,21,23] and assessed [24] data points. Present calculations are shown by solid lines, those of Wang et al. [13] by dotted lines and those of Zhang et al. [14] by dashed lines. The grey area is magnified in Figure 4
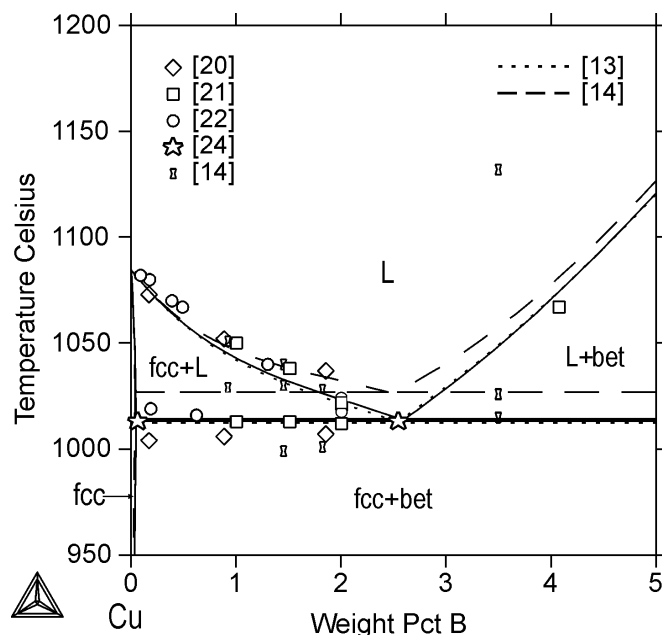

Fig. 4. Calculated Cu-rich portion of the B-Cu phase diagram (grey area of Fig. 3), with experimental [14,20-22] and assessed [24] data points. The present calculations are shown by solid lines, those of Wang et al. [13] by dotted lines and those of Zhang et al. [14] by dashed lines

tendency of the data of Zhang et al. [14] to favour the formation liquid miscibility gap at high temperatures (Fig. 3), in regard to the present results and those of Wang et al. [13].

In Figures 3 and 4, the calculations of this study and Zhang et al. [14] agree slightly better than those of Wang et al. [13] for the measured [25] mixing enthalpy data of liquid (Fig. 5) and for the measured [26] copper activity data in liquid (Fig. 6), whereas the calculations of this study and Wang et al. [13] agree slightly better than those of Zhang et al. [14] for the measured

[27] boron activity data in liquid (Fig. 4). In Figure 6, note also the poor agreement with the measured boron activities of [28] by any calculations.

3.2. System Fe-B-Cu

Figures 7-12 present the results obtained by the current optimization of the Fe-B-Cu system, which agree reasonably
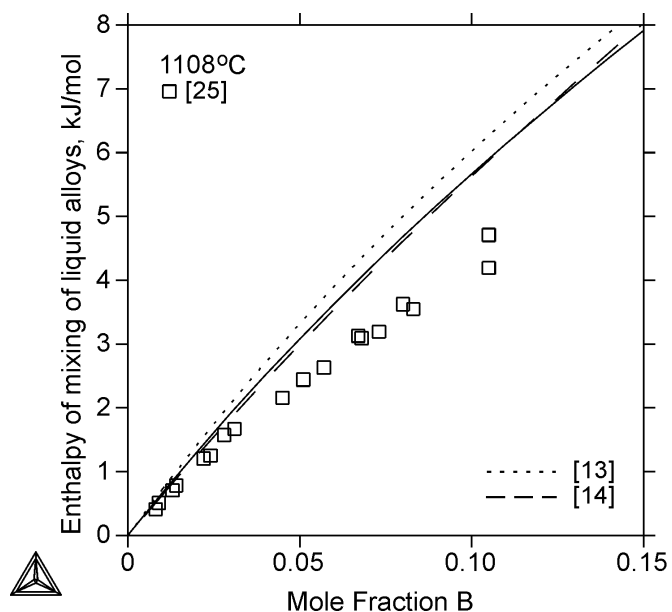
Fig. 5. The calculated enthalpy of mixing of liquid B-Cu alloys at 1,108°C, with experimental data points of Kleppa and Sato [25]. The present calculations are shown by solid lines, those of Wang et al. [13] by dotted lines and those of Zhang et al. [14] by dashed lines. The reference states used are pure liquid Cu and pure beta-rhombo B
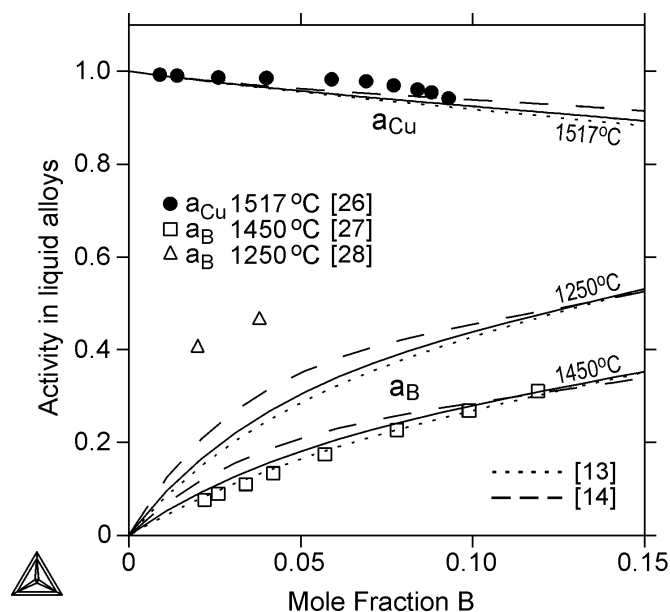

Fig. 6. The calculated activities of Cu and B in liquid B-Cu alloys, together with experimental data points of Batalin et al. [26], Jacob et al. [27] and Yukinobu et al. [28]. The present calculations are shown by solid lines, those of Wang et al. [13] by dotted lines and those of Zhang et al. [14] by dashed lines. The reference states used are pure liquid Cu and pure beta-rhombo B

well with the experimental data (Table 2). The calculated liquidus projection (Fig. 7) should be considered as tentative, due to the lack of systematic experimental data for the different liquidus surfaces. In addition, the calculated liquid miscibility gap may remain too stable at high temperatures. This is due to the strong temperature dependency of the liquid state ternary interaction parameter $L^{L}_{B,Cu,Fe}$ which was optimized using the measurements of Ono et al. [29] and Yamaguchi et al. [11]. In the iron-rich corner, two calculated

invariant points of reactions $L_1 + FeB = L_2 + Fe_2B$ (U) and $L_1 = L_2 + fcc + Fe_2B$ (E) are $1,380°C - 4.29wt\%Cu - 8.24wt\%B$ (U) and $1,175°C - 4.21wt\%Cu - 3.67wt\%B$ (E).

Figures 8-10 show the isothermal section of the system at 1,600°C (Fig. 8), its magnification in the iron-rich corner (Fig. 9) and the isothermal section of 1,250°C in the iron-rich corner (Fig. 10). The agreement is reasonable though note a slight discrepancy between the calculated and measured tie-lines at the Fe-Cu side of the system in Figure 9. Also note, in Figure 10,
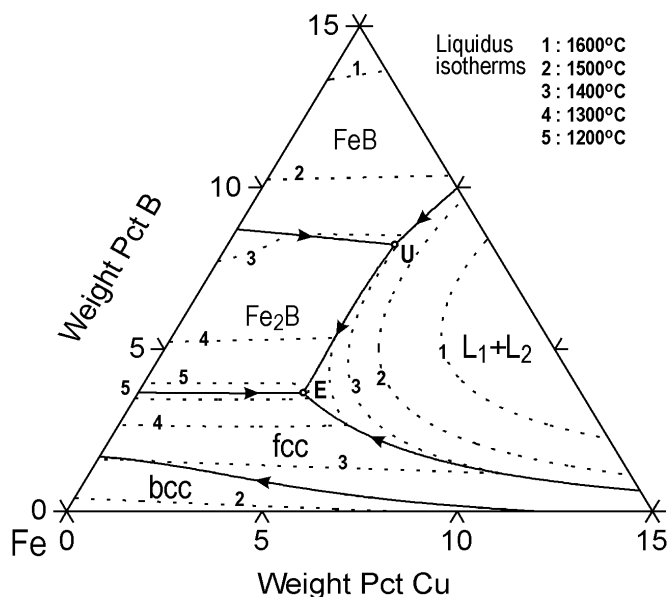

Fig. 7. The calculated liquidus projection in the Fe-rich corner of the Fe-B-Cu system. Shown also are the calculated liquidus isotherms between 1,600°C and 1,200°C (dotted lines)
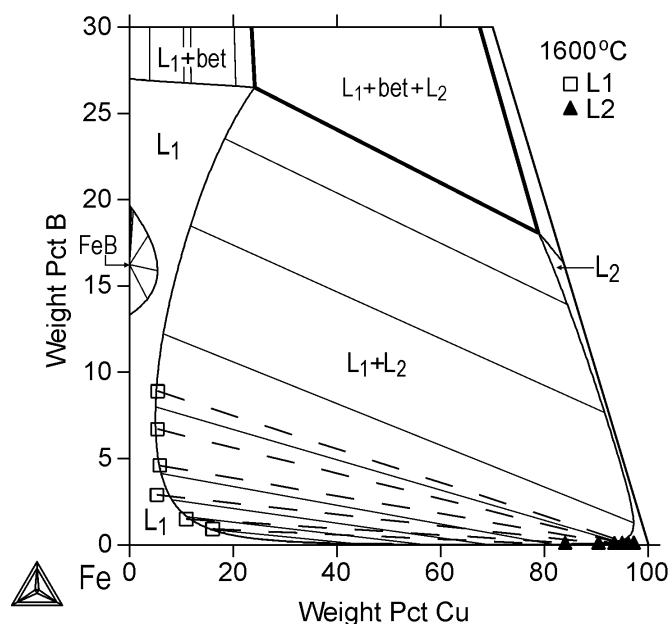

Fig. 8. The calculated isotherm of 1,600°C in the Fe-B-Cu system, with experimental data points of Ono et al. [29]
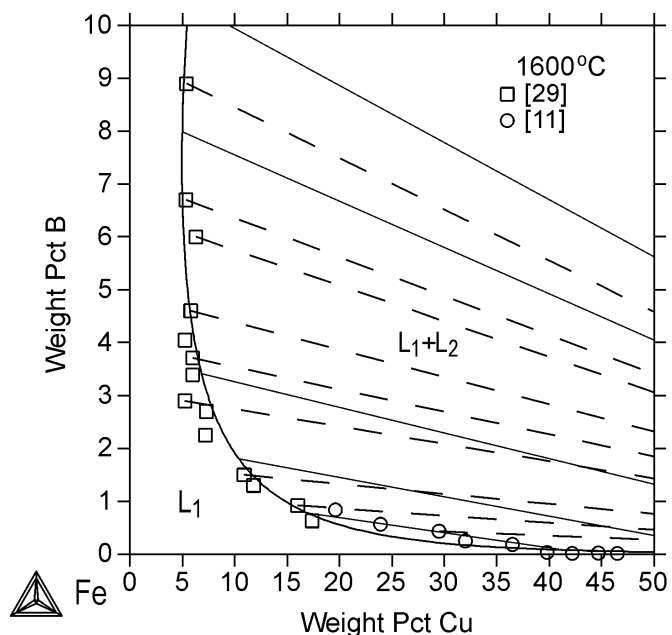
302

Fig. 9. The calculated isotherm of 1,600°C in the Fe-rich corner of the Fe-B-Cu system, with experimental data points of Ono et al. [29] and Yamaguchi et al. [11]
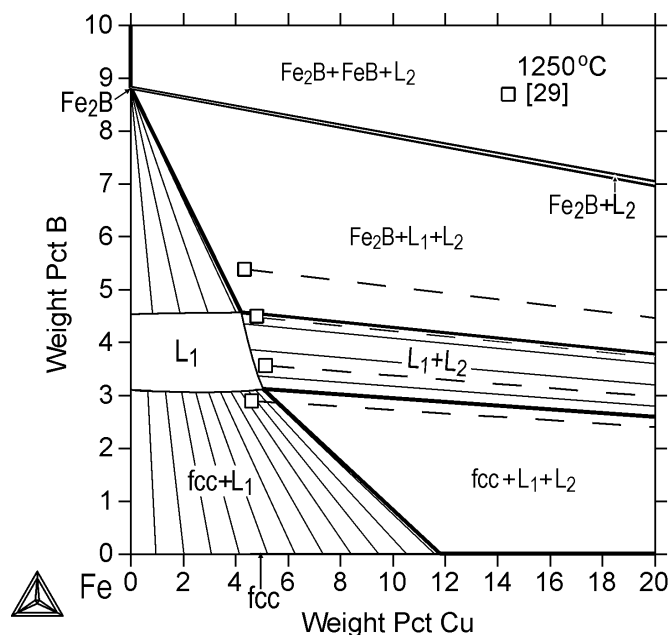

Fig. 10. The calculated isotherm of. 1,250°C in the Fe-rich corner of the Fe-B-Cu system, with experimental data points of Ono et al. [29]

the more stable liquid phase by the measurements of Ono et al. [29]. This is because of the low stability of the liquid phase by the Fe-B description of Miettinen and Vassilev [1].

In Figure 11, note the scattered experimental data of Ono et al. [29] and Yamaguchi et al. [11] for the activity coefficient f_{Cu}^{B} in liquid alloys. The agreement with calculations, however, can still be considered reasonable.

Figure 12 shows the calculated solubility of B in the fcc phase of the system. Increasing the Cu content and the tempera-

ture increases the B solubility in fcc. Note also that decreasing the temperature from 1,150°C to 1,000°C replaces the fcc + L_2 equilibrium with that of fcc + fcc_2.

An additional comparison was made for the phase equilibria of quaternary Fe-B-Cu-2.8wt%C alloys measured at 1,250°C by Taguchi et al. [33]. In these calculations, the earlier assessed Fe-B-C description [7] and the Fe-Cu-C description of the IAD database were combined with the present Fe-B-Cu description. As a result, reasonable accordance was obtained between the cal-
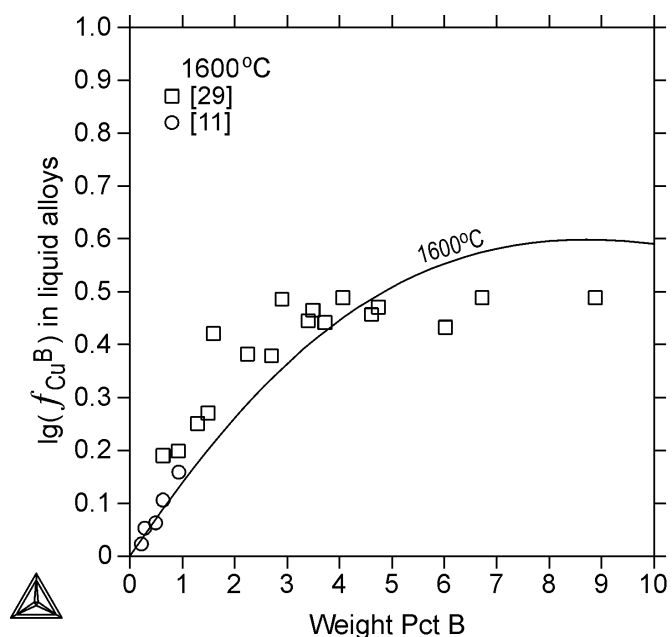

Fig. 11. The calculated activity coefficients of f_{Cu}^{B} in liquid Fe-B-Cu alloys at 1,600°C, with experimental data points of Ono et al. [29] and Yamaguchi et al. [11]
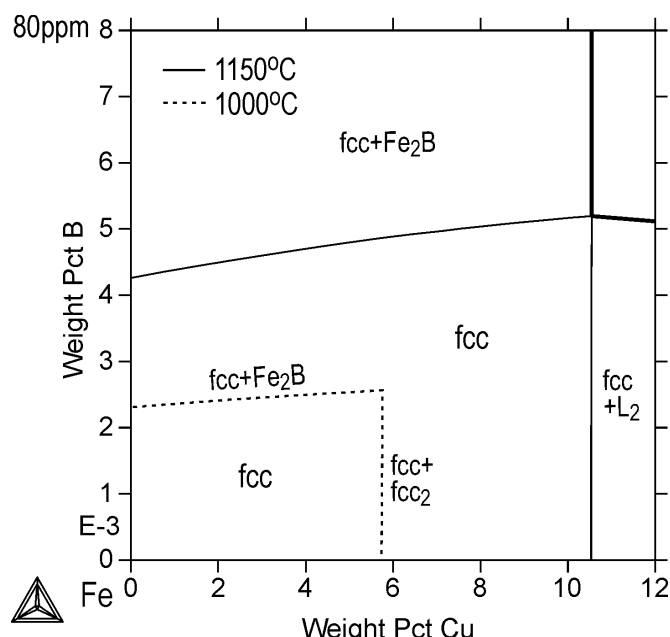

Fig. 12. The calculated solubility of B in the fcc phase of the Fe-B-Cusystem at 1,150°C and 1,000°C

culated and the measured copper solubility in the iron-rich liquid phase of the system, as shown in Figure 13. Note that the graphite phase not detected by Taguchi et al. [33] was suspended from the calculations. By allowing its presence (see the L_1/L_1 + gra boundary given by the broken line), only one experimental data point (owing composition 3.25 wt% B) is located in the liquid phase boundary of the liquid + graphite region.
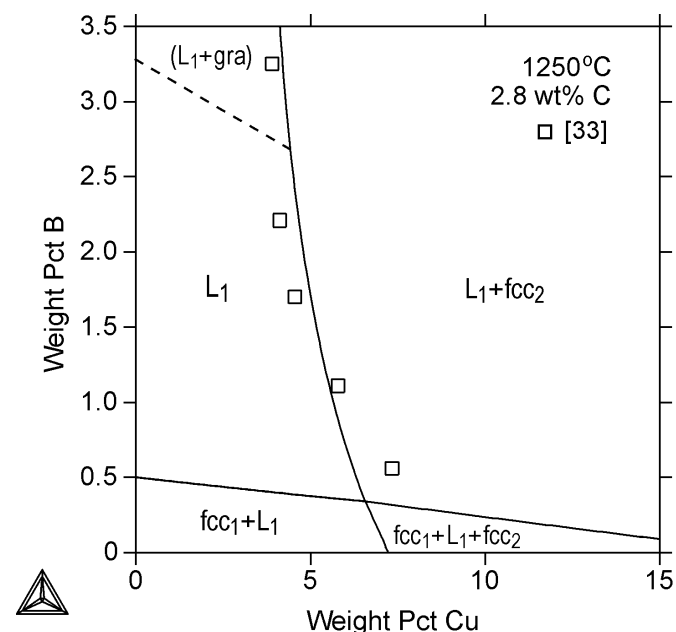

Fig. 13. The calculated isotherm of 1,250°C in the Fe-B-Cu-C system at 2.8 wt% C, with experimental data points of Taguchi et al. [33]. The experimentally undetected graphite was suspended from the calculations. Abbreviations fcc_1 and fcc_2 refer to Fe-rich and Cu-rich fcc phases, respectively

4. Conclusions

This work represents a step toward extending the thermodynamic Iron Alloys Database to be used to simulate the non-equilibrium solidification and solid-state phase transformations of steels. The thermodynamic descriptions of the Fe-B and Fe-Cu have been retained from already published sources. The parameters of the other binary sub-system, B-Cu, were reassessed. For the sake of consistency and simplicity of the whole database, it has been admitted that B forms substitutional solutions in the B-Cu and Fe-B-Cu systems. In these descriptions, six phases (i.e., liquid, bcc, fcc, β-rhombo-B, Fe_2B, and FeB) have been considered. Experimental thermodynamic and topological data have been used for the optimization of the B-Cu and Fe-B-Cu systems. The results indicate a good correlation between the calculated and experimental thermodynamic and phase equilibrium data. The new Fe-B-Cu description is valid for the entire composition range of the system, though only a partial validation of the boron-rich part of the system is provided due to the lack of suitable measurements.

REFERENCES

[1] J. Miettinen, G. Vassilev, Arch. Metall. Mater. **59**, 601-607 (2014).

[2] J. Miettinen, G. Vassilev, Arch. Metall. Mater. **59**, 609-614 (2014).

[3] J. Miettinen, K. Lilova, G. Vassilev, Arch. Metall. Mater. **59**, 1481-1485 (2014).

[4] J. Miettinen, V.-V. Visuri, T. Fabritius, N. Milcheva, G. Vassilev, Arch. Metall. Mater. **64**, 451-456 (2019).

[5] J. Miettinen, V.-V. Visuri, T. Fabritius, N. Milcheva, G. Vassilev, Arch. Metall. Mater. **64**, 1239-1248 (2019).

[6] J. Miettinen, V.-V. Visuri, T. Fabritius, N. Milcheva, G. Vassilev, Arch. Metall. Mater. **64**, 1249-1255 (2019).

[7] J. Miettinen, V.-V. Visuri, T. Fabritius, G. Vassilev, Arch. Metall. Mater. **65**, 923-933 (2020).

[8] J. Miettinen, V.-V. Visuri, T. Fabritius, Arch. Metall. Mater. **66**, 281-295 (2020).

[9] J. Miettinen, V-V. Visuri, T. Fabritius, Acta Univ. Oul. C, 704 (2019).

[10] J. Miettinen, S. Louhenkilpi, H. Kytönen, J. Laine, Math. Comput. Simulat. **80**, 1536-1550 (2010).

[11] K. Yamaguchi, H. Ono, T. Usui, Materials Trans. **51**, 1222-1226 (2010).

[12] Q. Chen, Z. Jin, Metall. Mater. Trans. A **26A**, 417-426 (1995).

[13] C.P. Wang, S.H. Guo, A.T. Tang, F.S. Pan, X.J. Liu, K. Ishida, J. Alloys Compd. **482**, 67-72 (2009).

[14] W.-W. Zhang, Y. Du, H. Xu, Y. Kong, W. Sun, F. Pan, A. Tang, J. Phase Equilib. Diff. **30**, 480-486 (2009).

[15] A. Dinsdale, A. Kroupa, A. Watson, J. Vrestal, A. Zemanova, P. Broz, COST action MP0602 -Handbook of High-Temperature lead-Free Solders – Atlas of Phase Diagrams, Vol. 1 ISBN 978-80-905363-1-9, Printed in the Czech Republic, 2012, pp 2018.

[16] A.T. Dinsdale, Calphad **15**, 317-425 (1991).

[17] O. Redlich, A.T. Kister, Ind. Eng. Chem. **10**, 345-348 (1948).

[18] Y.M. Muggianu, M. Gambino, P. Bros, J. Chim. Phys. **72**, 83-88 (1975).

[19] M. Hillert, M. Jarl, Calphad **2**, 227-238 (1978).

[20] F. Wald, R. Stormont, J. Less-Common Met. **9**, 423-433 (1965).

[21] J. Rexer, O. Petzow, Metall **24**, 1083-1086 (1970).

[22] A.P. Smiryagin, O.S. Kvurt, Tr. Gos. Nauchn. Issled. Proektn. Inst. Splav. Obrab. Tsvetn. Metall. **24**, 7-11 (1965)

[23] J.P. Piton, G. Vuillard, T. Lundström, C.R. Acad. Sci. C **278**, 1495-1496 (1974).

[24] D.J. Chakrabarti, D.E. Laughlin, in: Phase Diagrams of Binary Copper Alloys, P.R. Subramanian, D.J. Chakrabarti, D.E. Laughlin eds., ASM International, Materials Park, OH, USA, 1994, pp. 74-78.

[25] O.J. Kleppa, S. Sato, J. Chem. Thermodynamics **14**, 133-143 (1982).

[26] G.I. Batalin, V.S. Sudatsova, M.V. Mikhaiolvskaya, Izv. Vyssh. Ucheb. Zaved. Tsvetn. Metall. No.2, 125-127 (1985).

[27] K.T. Jacob, S. Priya, Y. Waseda, Metall. Mater. Trans. A **31**, 2674-2678 (2000).

[28] M. Yukinobu, O. Ogawa, S. Goto, Metall. Trans. B **20**, 705-710 (1989).

[29] H. Ono, K. Yamaguchi, S. Agawa, K. Taguchi, T. Usui, J. High. Temp. Soc. **35**, 40-44 (2009).

[30] B. Hallemans, Wollants, J.R. Roos, Z. Metallkd. **85**, 676-682 (1994).

[31] I. Ansara, A.T. Dinsdale, M.H. Rand, COST 507 – Thermochemical database for light metal alloys, Volume 2, European Communities, Belgium, 1998.

[32] J.-O. Andersson, T. Helander, L. Höglund, P. Shi, B. Sundman, Calphad **26**, 273-312 (2002)

[33] K. Taguchi, H. Ono-Nakazato, T. Usui, ISIJ Int. **46**, 633-636 (2006).